

Development of fast parallel multi-technique scanning X-ray imaging at Synchrotron Soleil

K. Medjoubi¹, N. Leclercq, F. Langlois, A. Buteau, S. Lé, S. Poirier,
P. Mercère, C. M. Kewish and A. Somogyi
Synchrotron Soleil, BP48 Saint-Aubin, Gif sur Yvette, 91192, France
E-mail: kadda.medjoubi@synchrotron-soleil.fr

Abstract A fast multimodal scanning X-ray imaging scheme is prototyped at Soleil Synchrotron. It permits the simultaneous acquisition of complementary information on the sample structure, composition and chemistry by measuring transmission, differential phase contrast, small-angle scattering, and X-ray fluorescence by dedicated detectors with ms dwell time per pixel. The results of the proof of principle experiments are presented in this paper.

1. Introduction

Scanning hard X-ray nanoprobe techniques provide the possibility of introducing several detectors around the sample (figure 1). As such, complementary information can be registered simultaneously while the sample is raster scanned in the focused beam; elemental maps can be obtained by using an energy-dispersive X-ray fluorescence (XRF) detector while the defocused beam is registered in transmission by a fast and sensitive two-dimensional (2D) detector providing differential phase contrast (DPC), dark field and transmission images.

The Nanoscopium hard X-ray nanoprobe beamline of Soleil will be dedicated to such multimodal scanning imaging in the 5 to 20 keV energy range [1]. It aims to offer 2D/3D quantitative information on the elemental state composition and electronic density of the sample with high spatial resolution and detection sensitivity. The targets are 30 nm in 3D spatial resolution, and parts-per-million (ppm) to parts-per-billion (ppb) trace element detection. Fast scanning imaging will allow the probing of large fields of view while high precision step-by-step scanning will provide precise local information. The main user communities of the beamline are biology, life sciences, geo-biology, and environmental sciences.

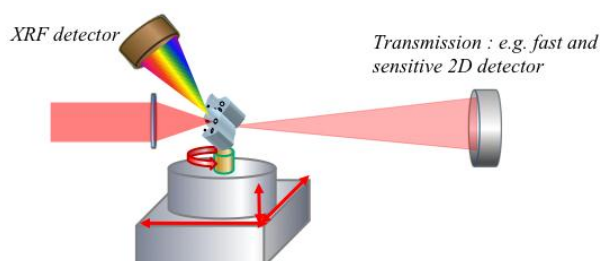


Figure 1. Principle of multi-technique scanning hard X-ray nanoprobe measurements. The X-rays are incident from the left, and the red arrows indicate the degrees of freedom in sample motion required for 3D imaging.

¹ Corresponding author.

Fast simultaneous data acquisition by high data through-put detectors with kHz readout frequencies results in large data volumes of the order of terabytes ($1 \text{ TB} = 2^{40}$ bytes) during a user experiment. In order to tackle the related technical challenges, a transverse project, named as FLYSCAN, has been prototyped at Synchrotron Soleil. The project aims to provide a flexible, general hardware and software architecture, which is adaptable to all Soleil beamlines for hardware-synchronized fast multi-detector experiments.

2. The FLYSCAN Architecture

The architecture of the FLYSCAN scheme is presented in figure 2. A hardware trigger signal synchronizes the acquisition of the detectors and the readout of the encoded motor positions. All these data are read out simultaneously at each pixel of the continuous scan with an exposure/dwell time determined by the period of the trigger signal.

The data collection of each detector is handled by its own independent TANGO device [2], which takes care of the data conversion and data output into temporary files. An asynchronous process, piloted by the Merger TANGO device, merges these temporary files and the metadata of the experiment conditions into a unique Nexus file [3]. The possibility of reading this file during the acquisition process permits on-line data processing. At the end of the acquisition, the final Nexus file is copied to the central storage space of Soleil, where it is available for off-line data processing.

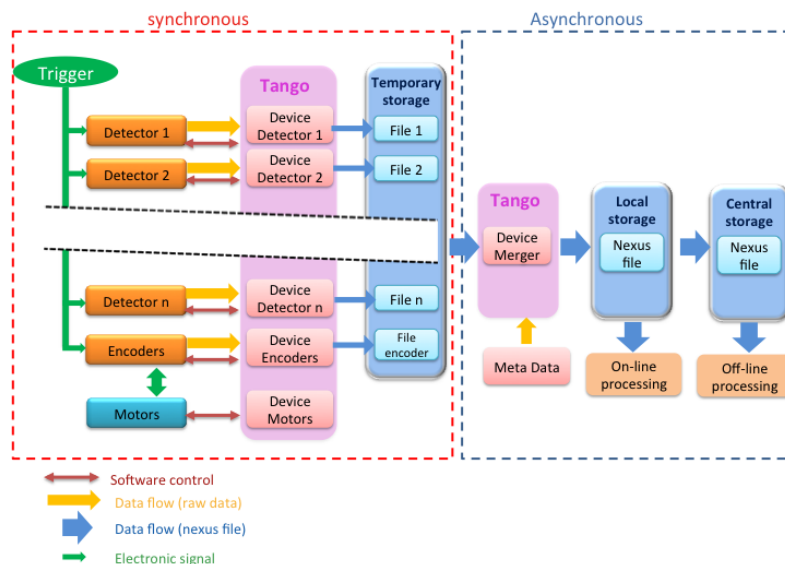


Figure 2.

Scheme of the FLYSCAN architecture developed for hardware synchronized multi-technique measurements, divided into synchronous and asynchronous processes.

3. Experimental set-up

Test experiments were carried out to demonstrate the feasibility of the FLYSCAN architecture, at the Metrologie bending magnet beamline [4] using a temporary scanning microprobe set-up. The 14 keV X-ray beam was focused by a Fresnel zone plate (FZP) into a $1.6 \mu\text{m}$ full-width at half-maximum (FWHM) measured beam size with 6×10^6 photons per second intensity.

During the experiments the XY sample positions transversal to the beam were recorded for each trigger signal. The corresponding defocused transmitted beam pattern was measured at each scan position by a photon counting pixel detector placed 4.41 m behind the sample. The single module XPAD [5] detector has a $500 \mu\text{m}$ -thick silicon sensor composed of 120×560 array of $130 \times 130 \mu\text{m}^2$ pixels, which can be read out as a full frame in 1.6 ms.

The X-ray fluorescence (XRF) signal emitted by the sample was detected by a silicon drift detector (SDD) having 80 mm^2 active area (VITUS H80, KETEK GmbH). The detector was placed perpendicularly to the incident beam in the horizontal plane to minimize the detection of elastic X-ray scattering from the sample. A high-speed digital multichannel analyser (MCA) (xMAP, XIA LLC) was used in double-buffering mode to process the signal of the SDD.

A $5 \mu\text{m}$ thick silicon photodiode (AXUV36, IRD Inc.) was used to monitor the flux of the incident beam, for data normalization. The counter card, the XPAD, the xMap and the ADC

were controlled by their own TANGO devices. The data acquisition of each device was started by an external trigger signal.

The sample was scanned using a continuous scan in the horizontal direction while step scan mode was used in the vertical direction. In order to reduce further the total scanning time we performed bi-directional horizontal scans.

In each pixel of the reconstructed images, the DPC, the transmission and the dark field information were obtained from the recorded XPAD frame [6]. The DPC was obtained by calculating the centroid of the illumination pattern. The transmission was given by the total intensity recorded in the image. The dark field was evaluated by integrating the scattered intensity, outside the first order beam. Elemental maps were obtained from the intensities of selected fluorescence peaks, defined by integrating regions of interest (ROIs) of the XRF spectra. Each reconstructed image was rescaled by the recorded encoder positions to correct for motor acceleration/deceleration, and backlash.

4. Results

Large field of view fast scanning imaging has been demonstrated on a food moth (figure 3a) by measuring an image of 1000×1000 pixels. The pixel size is $1.6 \times 2 \mu\text{m}^2$. We used 12 ms dwell time/pixel, comprising 10 ms exposure time, required to obtain sufficient intensity in the XPAD image, and 2 ms readout time. The obtained data set consists of one million XPAD frames and intensity monitor values, and 2 million motor positions. All the data are merged into a single Nexus file of 140 Gbytes.

The vertical DPC images, both uncorrected and with encoder position correction are shown in figures 3b and 3c, respectively. The phase map was reconstructed from the vertical and

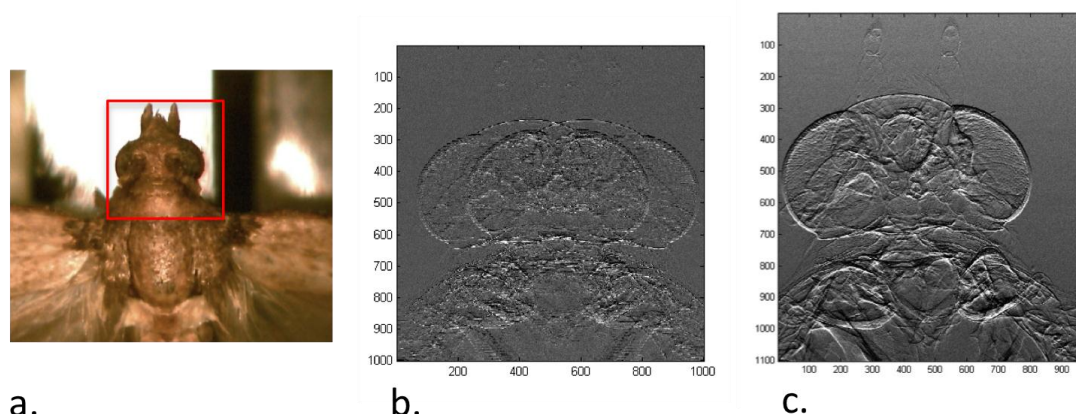


Figure 3. Scanning X-ray images of the head of a moth using the FLYSCAN scheme. The scanned area is indicated by the red rectangle in Fig 3a. Vertical differential phase contrast image, before (Fig. 3b) and after (Fig. 3c) correcting with the encoded motor positions. For scale reference, the width of images (b-c) is 1.6 mm.

horizontal DPC images using a Fourier integration technique [7]. Further details on the phase, transmission, DPC, and dark field images can be found in Medjoubi et. al. [8].

Simultaneous multi-technique fast scanning imaging was performed by the XPAD and the SDD detectors. The test sample was a copper wire of $230 \mu\text{m}$ diameter containing an insulating sheath. The simultaneously recorded absorption, DPC, dark field and XRF maps can be seen in Figure 4. The image contains 500×500 pixels with $2.6 \times 2 \mu\text{m}^2$ pixel size. The dwell time/pixel was 22 ms (20 ms exposure time and 2 ms readout). The total acquisition time including communication and data storage overhead was ~ 1 hour.

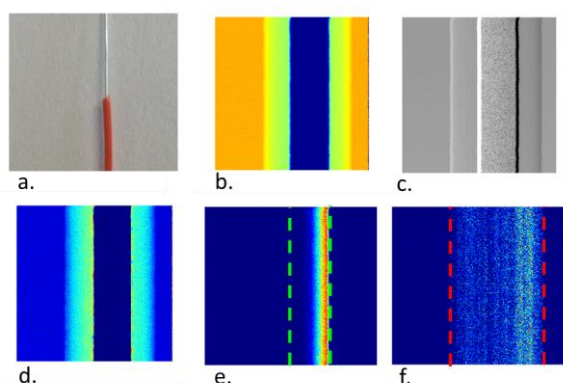


Figure 4. (a) Photograph of insulated copper wire, (b) transmission, (c) horizontal DPC, (d) dark field image, (e) copper, and (f) selenium distribution. The dashed lines represent the edges of the wire and the insulating sheath. For scale reference, the width of images (b-f) is 1 mm.

Figures 4b, 4c and 4d show the measured transmission, DPC, and dark field images. The images have been corrected with the recorded encoder positions. In the Cu map shown in figure 4e the self-absorption of the Cu-K α fluorescence line is evident. Selenium is distributed in-homogenously in the insulating sheath, the line structures of the sheath and the self-absorption effect is clearly visible (Figure 4f).

5. Conclusion

A fast, parallel multi-technique continuous scanning scheme has been developed and tested at Synchrotron Soleil. The FLYSCAN architecture ensures the flexible integration of individual, externally triggered detectors, each of which is controlled by its own TANGO device. The minimum dwell time available in our current scheme was 1.6 ms, limited by the XPAD detector readout time.

We demonstrated the collection of large field of view images by the FLYSCAN scheme. The measured data and metadata are recorded in a single Nexus file. On-line data processing during the acquisition is possible for data visualisation. The simultaneous recording and combining of X-ray fluorescence, absorption, phase contrast and dark field images opens the possibility for quantification [9].

Acknowledgement

The authors are grateful to G. Baranton and P. Da Silva from Soleil for their assistance with the synchrotron experiments, and to the XPIX collaboration (SOLEIL/CPPM-CNRS/Neel Institute) providing the XPAD detector. We acknowledge V. Kaiser (ANKA / Softwareschneider GmbH) for providing the xMAP TANGO device and our colleagues from the Controls groups ICA/ECA from Soleil who helped with the test experiments.

References

- [1] Somogyi, A., Kewish, C. M., Polack, F., & Moreno, T. (2011), *AIP Conf. Proc.*, **1365**, 57-60
- [2] <http://www.tango-controls.org>
- [3] Poirier, S., Maréchal, C., Ounsy, M., Buteau, A., Martinez, P., Gagey, B., Pierrot, P., Mederbel, M., & Rochat, J. M., (2009). *Proceedings of ICALEPCS09*, Kobe, Japan
- [4] Idir, M., Mercere, P., Moreno, T., Delmotte, A., Dasilva, P. and Modi, M.H. (2010). *AIP Conf. Proc.*, **1234**, 485-488.
- [5] Medjoubi, K., Bucaille, T., Hustache, S., B éar, J. F., Boudet, N., Clemens, J. C., Delpierre, P., & Dinkespiller, B. (2010). *J. Synchrotron Rad.* **17**(4), 486-495.
- [6] Menzel, A., Kewish, C. M., Kraft, P., Henrich, B., Jefimovs, K., Vila-Comamala, J., David, C., Dierolf, M., Thibault, P., Pfeiffer, F., and Bunk, O. (2010). *Ultramicroscopy*, **110**, 1143-1147.
- [7] Kottler, C., David, C., Pfeiffer, F. & Bunk, O. (2007). *Opt. Express*, **15**, 1175-1181.
- [8] Medjoubi, K., Leclercq, N., Langlois, F., Buteau, A., L é S., Poirier, S., Merc ère, P., Sforza, M., Kewish, C. M. & Somogyi, A. (2012) submitted
- [9] Kosior, E., Bohic, S., Suhonen, H., Ortega, R., Dev ès, G., Carmona, A., Marchi, F., Guillet, J.F., Cloetens, P. (2012), *Journal of Structural Biology*, **177**, 239–247